

AN INSIGHT INTO THE PYROPLASTICITY OF PORCELAIN STONEWARE TILES

**Fábio G. Melchiades ⁽¹⁾, Anselmo O. Boschi ⁽¹⁾,
Lisandra R. dos Santos ⁽¹⁾, Michele Dondi ⁽²⁾, Chiara Zanelli ⁽²⁾,
Mariano Paganelli ⁽³⁾, Vittorio Mercurio ⁽³⁾**

⁽¹⁾ LaRC, Laboratório de Revestimentos Cerâmicos, Departamento de Engenharia de Materiais, Universidade Federal de São Carlos, Brazil

⁽²⁾ CNR-ISTEC, Istituto di Scienza e Tecnologia dei Materiali Ceramici, Faenza, Italy

⁽³⁾ Expert System Solutions, Modena, Italy

ABSTRACT

Pyroplasticity is active when sintering acts through viscous flow of an abundant amorphous phase, as typical of porcelain stoneware. It has become increasingly important in ceramic tile making with the development of large sizes, rectangular shapes, low thickness, and with use of vigorous fluxes and micronized fillers. Firing deformations are thought to depend on the amount, size, shape and mutual arrangement of coarse grains, as well as on the viscosity of the liquid phase that forms at high temperature. The objective of the present work was to identify the main variables responsible for the pyroplastic index and to suggest alternatives to reduce it. An insight into the pyroplasticity of porcelain stoneware tiles was gained by substituting raw materials in a typical industrial-like body composition. The six compositions were prepared by wet milling and sieve granulation. Bodies and green compacts were characterized by determining the chemical composition, particles size and green bulk density. Fired samples were characterized by determining the water absorption, bulk density, open and closed porosity, and phase composition (XRD-Rietveld). Firing deformation was determined by both the three-point flexural test at maximum density temperature (expressed as the pyroplasticity index and uniaxial viscosity) and by the Fleximeter (maximum deflection). Results showed that pyroplasticity was significantly affected by the nature of the vitreous phase at the temperature of the maximum densification rate (viscosity and flow point) and was not correlated with the volume of the vitreous phase.

1. INTRODUCTION

The term “pyroplasticity” is commonly used to refer to deformations occurring during the firing of whitewares[1]. It has become increasingly important in ceramic tile making with the development of larger sizes, rectangular shapes, lower thickness, and with the use of vigorous fluxes and micronized fillers, particularly when two or more of these factors are combined in the same production[2-3].

There is a large body of literature on creep of oxide ceramics; however, comparatively very little has been published on the high temperature deformations of ceramic tiles, or “pyroplasticity”, a term commonly used to refer to deformations occurring during the firing of whitewares[1]. This phenomenon is active when sintering acts through the viscous flow of an abundant amorphous phase, as typical of porcelain stoneware[4]. Pyroplasticity is thought to depend on the amount, size, shape and microstructural arrangement of coarse grains (the so-called ‘skeleton’), as well as on the physical properties of the amorphous phases at high temperature (especially viscosity)[5-9].

The objective of the present work was to identify the main variables responsible for the pyroplastic index, the usual manner to quantitatively express this phenomenon, and to suggest alternatives to reduce it.

3. EXPERIMENTAL

Compositions	51	52	53	54	55	56
Raw material (wt %)						
Kaolin	25	25	25	25	25	25
Ball clays	12	12	12	12	12	12
Bentonite	4	4	4	4	4	4
Talc	4	4	4	4	4	4
Zircon	3	3	3	3	3	3
Na Feldspar C	26	21	21	21	21	21
Na-K Feldspar C	26	21	21	21	21	21
Quartz C		10			5	
Quartz F			10			5
K Feldspar F				10	5	5

Table 1. Body formulations (C=coarse, F=fine).

As shown in Table 1, to study the effect of the body formulation on the pyroplastic deformation of porcelain stoneware tiles, six compositions were produced. Composition 51 is a standard formulation that was modified by replacing 10% of the coarse-grained feldspars, usually utilized in the ceramic industry, with other raw materials. These changes were designed to establish the effect of the chemical/mineralogical and physical characteristics (particle size) of the different raw materials. In compositions 52 and 53, the feldspar was replaced with coarse (Quartz C) and fine (Quartz F) quartz, respectively. In composition 54 the feldspar was replaced with fine grained potassium feldspar (K Feldspar F). In compositions 55 and 56 a combination of the previous changes was made.

The chemical compositions of the bodies were determined by XRF. Loss on ignition was evaluated at 1000°C.

Body preparation entailed wet grinding in ball mills with 50% water and 0.6% sodium silicate (deflocculant). The residue content was controlled between 0.5% and 2.0% after sieving through an ASTM #325-mesh sieve (45 μm).

Prismatic test specimens were prepared by pressing at 450 kgf/cm². The moisture content of the powders was previously adjusted to 6.5%.

Bulk density of unfired compacts was determined by geometric measurements to evaluate the apparent volume of the dried test specimens. Drying was performed in an electric oven at 110°C.

Sintering curves were obtained by evaluating the water absorption and linear shrinkage after firing to four different maximum temperatures. The heating rate was 60°C/min and the soaking time at the maximum temperature was 8 minutes. The sintering curves were employed to determine the maximum densification temperature (T_{md}) corresponding to the highest linear firing shrinkage of the samples.

Specimens fired at T_{md} were characterized by measuring: water absorption WA, open porosity OP, and bulk density, BD (ISO 10545-3); total porosity as $TP = 100 \times (1 - BD/SW)$ where the specific weight, SW, was determined by He pycnometry (ASTM C-329); closed porosity as $CP = TP - OP$; phase composition was determined by X-ray diffraction (Bruker D8 Advance, 10-80°2 θ range, scan rate 0.02°, 16 s per step) with full profile interpretation by RIR-Rietveld refinement (GSAS-EXPGUI) [10].

The chemical composition of the vitreous phase was derived from the bulk chemical and phase composition of the samples and used to estimate the physical properties of the vitreous phase at high temperature (viscosity, surface tension) and room temperature (density) according to the additive model[4].

Firing deformation was determined by two methods: 1) the three-point flexural test at maximum densification temperature (T_{md} , for 8-minute soaking time) and 2) the Expert System Solutions Fleximeter (30°C/min up to 1205°C, 5-minute soaking time) [11].

Results are expressed as:

- pyroplastic index (PI), in cm^{-1} , as $\text{PI}=(4 \cdot h^2 \cdot S) \cdot (3 \cdot L^4)^{-1}$, where h is the specimen thickness, S is the sag of the deformed specimen and L is the span length.
- uniaxial viscosity, in $\text{Pa} \cdot \text{s}$, as $E_p=(5 \cdot \text{BD} \cdot g \cdot L^4) \cdot (32 \cdot \delta_{\text{max}} \cdot h^2)^{-1}$, where g is the gravitational acceleration and δ_{max} the maximum deflection rate [12].

Results of the fleximeter are expressed as maximum deflection d in parallel with PI, calculated as deflection at T_{md} plus $\delta_{\text{max}} \cdot 480$ s to account for the soaking time.

Formulations	51	52	53	54	55	56	e.u.
Bulk density (g cm^{-3})	1.830	1.838	1.801	1.803	1.770	1.829	± 0.002

Table 2. Bulk density of the green compacts.

e.u. = experimental uncertainty

4. RESULTS AND DISCUSSION

The analysis of the results was done in two parts with complementary objectives. The objective of the first part was to identify the main variables responsible for determining the pyroplastic index of a porcelain stoneware tile composition. The objective of the second part was to look for explanations for the different behaviours of the studied compositions during firing.

4.1. FIRST PART: IDENTIFICATION OF THE MAIN VARIABLES

In accordance with the literature the variations of the body compositions produced by the partial substitution of the feldspar in the standard composition should affect three very important variables for the pyroplastic deformation of porcelain stoneware tiles: 1) bulk density, which establishes the volume available to accommodate the liquid phase; 2) the amount of liquid phase at the maximum densification rate, and 3) the nature of the liquid phase.

	Property	unit	51	52	53	54	55	56	e.u.
T_{md}	Maximum densification temperature	$^{\circ}\text{C}$	1185	1195	1190	1170	1185	1185	± 2
PI	Pyroplasticity index [3]	$\text{cm}^{-1} (10^{-5})$	9.5	8.4	7.8	9.1	8.6	7.4	± 0.1
E_p	Uniaxial viscosity [11]	$\text{MPa} \cdot \text{s}$	199	224	238	202	217	252	± 4
δ	Maximum deflection	$\text{cm} \cdot \text{m}^{-1}$	17.6	12.4	11.6	20.2	13.5	14.2	± 0.3
WA	Water absorption	wt%	0.01	0.01	0.17	0.08	0.08	0.16	± 0.02

OP	Open porosity	vol.%	0.1	0.1	0.4	0.2	0.2	0.4	±0.1
CP	Closed porosity	vol.%	6.6	4.4	3.4	4.7	6.8	5.0	±0.1
TP	Total porosity	vol.%	6.7	4.5	3.8	4.9	7.0	5.4	±0.1
SW	Densidad real	g·cm ⁻³	2.652	2.600	2.571	2.592	2.647	2.601	±0.005
BD	Bulk density	g·cm ⁻³	2.475	2.482	2.473	2.465	2.463	2.460	±0.005

Table 3. Pyroplastic indexes and physical features of fired bodies.

e.u. = experimental uncertainty

Thus in the sequence we will look for correlations between the bulk densities before firing, the vitreous phase volumes and the nature of the vitreous phase, and the Pyroplastic Index (PI).

As expected, the substitutions of the raw materials led to variations of the bulk density of the compacts, pressed at a fixed pressure (Table 2).

wt%	51	52	53	54	55	56	e.u.
SiO ₂	66.98	69.42	69.42	66.10	67.75	67.75	±0.25
ZrO ₂	2.06	2.05	2.05	2.05	2.05	2.05	±0.02
TiO ₂	0.31	0.31	0.31	0.31	0.31	0.31	±0.01
Al ₂ O ₃	22.44	21.25	21.25	23.11	22.18	22.18	±0.20
Fe ₂ O ₃	0.85	0.83	0.83	0.83	0.83	0.83	±0.02
MgO	1.89	1.73	1.73	1.73	1.73	1.73	±0.02
CaO	1.35	1.05	1.05	1.06	1.06	1.06	±0.02
Na ₂ O	3.39	2.68	2.68	2.98	2.83	2.83	±0.02
K ₂ O	0.70	0.63	0.63	1.79	1.21	1.21	±0.02
P ₂ O ₅	0.03	0.03	0.03	0.04	0.04	0.04	±0.01
Quartz	17.0	21.0	17.0	14.0	18.0	16.0	±0.5
Mullite	13.0	12.0	11.0	11.0	13.0	12.0	±0.5
Feldspar	2.0	2.5	2.0	2.0	2.5	3.0	±0.25
Zircon	3.0	2.5	2.0	3.0	2.5	2.0	±0.25
Vitreous phase	65.0	62.0	68.0	70.0	64.0	67.0	±1.0

Table 4. Chemical and phase composition of the samples after firing.

e.u. = experimental uncertainty

Oxide/property	unit	51	52	53	54	55	56	e.u.
SiO ₂	wt%	67.7	68.7	69.7	66.7	68.2	68.3	±0.5
TiO ₂	wt%	0.5	0.5	0.5	0.4	0.5	0.5	±0.1
ZrO ₂	wt%	0.0	0.4	0.8	0.0	0.4	0.9	±0.1
Al ₂ O ₃	wt%	19.6	19.7	19.1	21.2	19.4	19.4	±0.3
Fe ₂ O ₃	wt%	1.3	1.4	1.2	1.2	1.3	1.3	±0.2
MgO	wt%	2.9	2.8	2.5	2.5	2.7	2.6	±0.2
CaO	wt%	2.1	1.7	1.6	1.5	1.7	1.6	±0.2
Na ₂ O	wt%	4.9	3.9	3.6	3.9	4.0	3.7	±0.2
K ₂ O	wt%	1.1	1.0	0.9	2.6	1.9	1.8	±0.1
Viscosity at T _{md} ^[L]	kPa·s	4.75	4.77	4.80	4.97	4.78	4.81	±0.02
Flow Point ^[F] (viscosity: log ₁₀ =4)	°C	1192	1221	1231	1216	1210	1222	±2
Littleton Point ^[F] (viscosity: log ₁₀ =6.6)	°C	911	931	937	924	921	930	±2
Density at room T ^[B]	g·cm ⁻³	2.441	2.435	2.431	2.441	2.439	2.442	±0.005
Surface tension at T _{md}	mN·m ⁻²	357	356	354	357	354	354	±1

Table 5. Chemical composition and estimated physical properties of the vitreous phase.

e.u. = experimental uncertainty

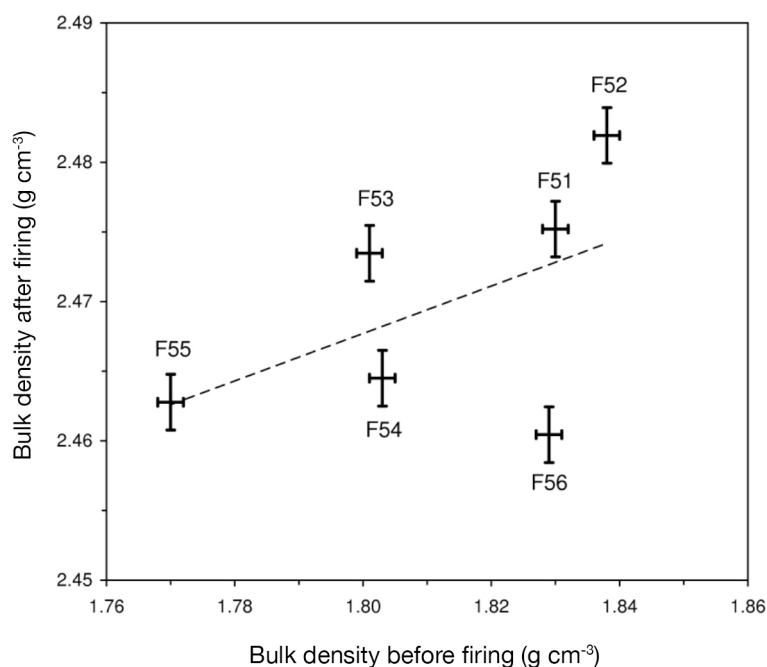


Figure 1. Effect of bulk density before firing on bulk density after firing at the maximum densification temperature.

Effect of bulk density before firing on the pyroplastic index (PI)

The bulk density after firing was influenced by the bulk density before firing (Figure 1). However composition 56, and to a lesser extent 54, deviated from the main trend. There was no clear correlation between the bulk density and the pyroplastic index (PI). This is not a surprise because the variation of the bulk density was due to important chemical, mineralogical and particle size changes and it would be impossible to separate the effects of all these alterations.

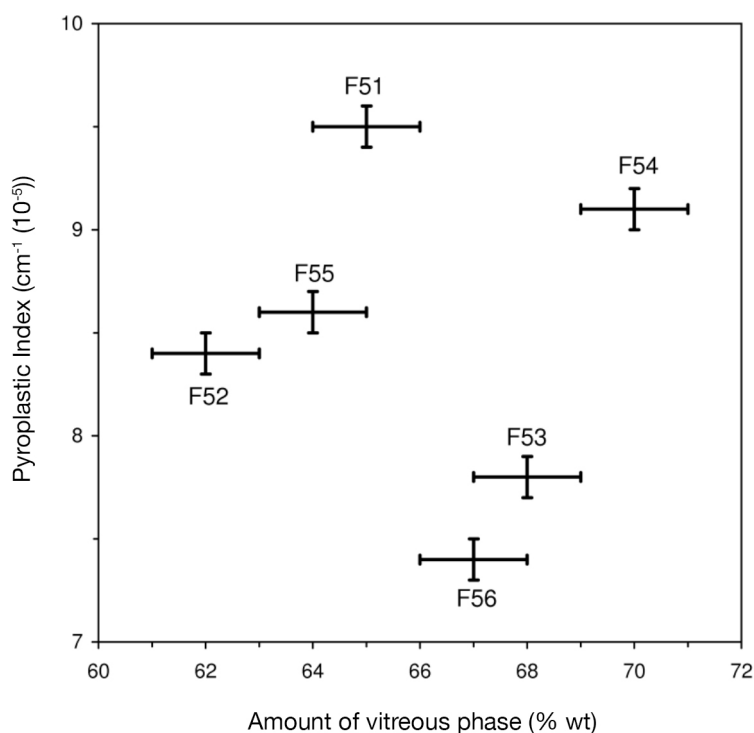


Figure 2. Effect of the amount of vitreous phase on the Pyroplastic Index (PI).

Effect of the volume of vitreous phase on the pyroplastic index (PI)

Figure 2 presents the result of an attempt to correlate the volume of the vitreous phase (Table 4) with the pyroplastic index (PI). As can be clearly seen, by the results of this work, these variables are not directly related.

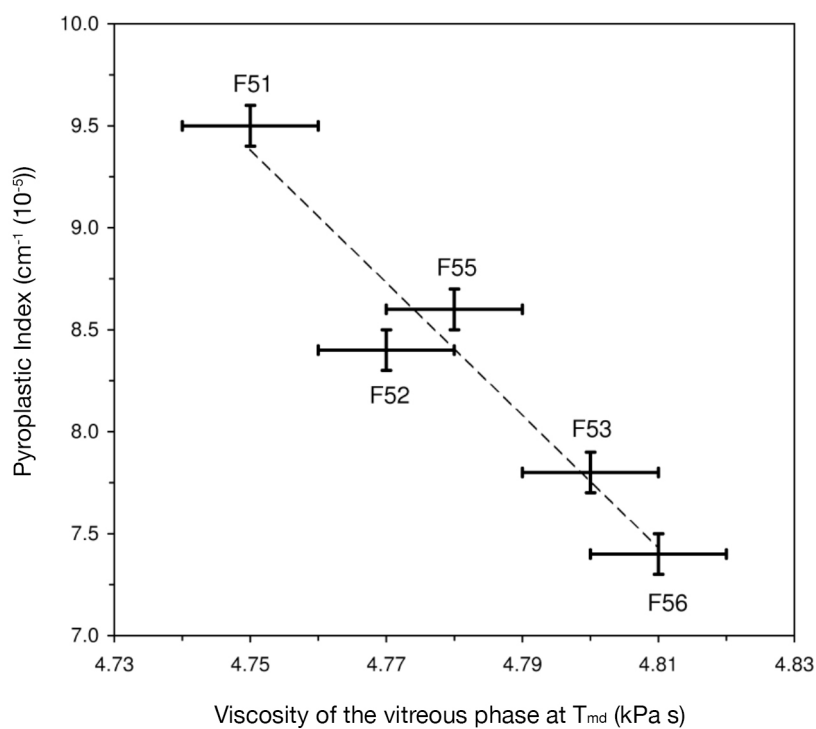


Figure 3. Effect of the viscosity of the vitreous phase at the maximum densification temperature on the pyroplastic index (PI), without the results of composition 54.

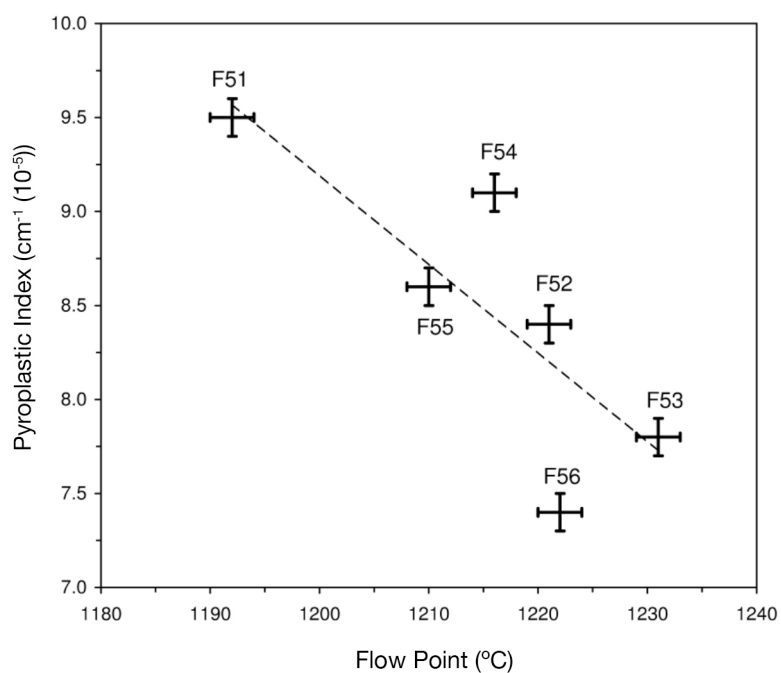


Figure 4. Effect of the flow point of the vitreous phase at the maximum densification temperature (T_{md}) on the pyroplastic index (PI).

Effect of the nature of vitreous phase on the pyroplastic index (PI)

To characterize the nature of the vitreous phase we will use some of the data presented in Table 5.

As can be seen in Figures 3 and 4, there is a very good correlation between the viscosity and the flow point of the vitreous phase at the maximum densification temperature (T_{md}) and the pyroplastic index (PI). It is important to mention that Figure 3 does not contain the result of composition 54 because it deviates from the main trend. A possible explanation for such a behaviour is likely to lie in the different ratio of feldspathic fluxes to the skeleton (quartz).

The results presented above suggest that, for the conditions of this work, the nature of the liquid phase at the maximum densification temperature is the most important variable in defining the pyroplastic index of porcelain stoneware tiles.

4.2. SECOND PART: SINTERING BEHAVIOUR OF THE DIFFERENT COMPOSITIONS

Effect of the composition variation on the maximum densification temperature

The maximum densification temperature (T_{md}) varied between 1170 and 1195°C. The substitution of 10% feldspar by quartz (51 and 52) increased T_{md} . The T_{md} for the coarser quartz was slightly higher. The substitution of part of the feldspar by a finer one led to a decrease of T_{md} and the combined substitutions in 55 and 56 resulted in the same T_{md} of the standard composition (51) (Table 3).

Composition 52 required the highest T_{md} to achieve $WA < 0.5\%$.

The particular importance of T_{md} for porcelain stoneware is due to the requirement of water absorption (WA) values smaller than 0.5%. However, it is important to mention that WA does not take into consideration closed pores (CP) and, as can be seen in Table 3, the variation of the volume of closed pores was quite significant. There is no straight correlation between CP and PI.

The effects of the substitution of 10% feldspar of the standard composition (51) on the firing behaviour, as evaluated by T_{md} , were as expected (Table 3). In fact, the maximum densification temperature increased by replacing feldspar with quartz (52 and 53) and this increment is higher for the coarser quartz. The substitution of coarse feldspar by fine feldspar (54) resulted in a decrease of T_{md} . No appreciable changes of T_{md} were registered for the other substitutions (54, 55 and 56).

Despite the variation of T_{md} , all the samples exhibited high bulk densities after firing and the range of variation was quite small (2.46-2.48 g·cm⁻³) (Table 3). The residual porosity, almost all closed pores, was approximately between 4% and 7%.

Effect on the phase composition at the maximum densification temperature

The major phase present after firing was the vitreous phase (from 62% to 70%). The major crystalline phases were quartz (14-21%) and mullite (11-13%). Minor amounts of feldspar (plagioclase) and zircon also were present (Table 4).

This phase composition appears to be coherent with the substitutions in the standard composition: for instance, the replacement of 10% coarse feldspar with coarse quartz (52) resulted in an increase in residual quartz and a decrease in vitreous phase content after firing. In composition 53, when the same amount of feldspar was substituted by fine quartz, the quartz content after firing was the same as that of the standard composition (51) in which quartz was not added as an individual raw material, but was present in the used raw materials, suggesting that the added fine quartz was almost completely dissolved by the vitreous phase. That would explain the increase in the vitreous phase content (Table 4) and the increase of viscosity at T_{md} and the flow point (Table 5).

The substitution of 10% coarse feldspar by a finer one (54) resulted, as expected, in a reduction of the quartz content and an important increase in amount of vitreous phase (Table 4). The combined substitutions in compositions 55 and 56 have intermediate effects. Composition 55 behaves approximately midway between 51 and 52, while composition 56 falls somehow between 51 and 53 (Table 4). Further crystalline phases present in the fired bodies – i.e. mullite, zircon and feldspar – are little affected by the changes in batch composition, since the variations observed are close to the experimental uncertainty.

5. CONCLUSIONS

The Pyroplastic Index varied from 7.4 to $9.5 \cdot 10^{-5} \text{ cm}^{-1}$, denoting a significant difference in the behaviour of the samples under investigation; that makes it possible to have an insight into high temperature deformations also at this preliminary stage of our study.

The Pyroplastic Index does not exhibit any clear correlation with physical properties of tiles: PI data plot into a cloud once contrasted with total porosity or bulk density (before and after firing). A direct relationship of PI with the amount of vitreous phase was expected, but it is in reality not significant in the samples under investigation.

For the conditions of this work, pyroplasticity seems to be more affected by the quality than by the quantity of the vitreous phase. In particular, its viscosity and tendency to flow at the maximum firing temperature of porcelain stoneware tiles. Interestingly, the Pyroplastic Index exhibits an inverse correlation with the Flow Point and the viscosity of the vitreous phase. These relationships indicate that the higher the temperature at which the glass begins to flow or the higher the viscosity of the vitreous phase at T_{md} , the lower the pyroplastic deformation. This is to a large extent expected, but never supported before by experimental data for porcelain stoneware. However, the sample F54 acts as an outlier, implying that such a simple dependence does not always apply and the subject requires further investigation to be fully understood.

The particle size determines whether the raw material will constitute a phase of its own or will be dissolved and incorporated into the liquid phase, altering its composition and behaviour. Thus, the use of fine raw materials that would increase the viscosity of the liquid phase at the temperature of the maximum densification rate will result in a reduction of the pyroplastic index.

REFERENCES

- [1] Buchtel A.M., Carty W.M., Pyroplastic deformation revisited. *Ceram. Eng. Sci. Proc.*, 25 [2] (2004) 25-42.
- [2] Raimondo M., Dondi M., Zanelli C., Guarini G., Gozzi A., Marani F., Fossa L., Processing and properties of large-sized ceramic slabs. *Boletín de la Sociedad Española de Cerámica y Vidrio*, 49 [4] (2010) 307-314.
- [3] Melchiades F.G., dos Santos L.R., NASTRI S., BOSCHI A.O., Gres porcelánico esmaltado producido por vía seca: materias primas fundentes. *Bol. Soc. Esp. Ceram. Vidr.* Vol 51. 2, 133-138.
- [4] Zanelli C., Guarini G., Raimondo M., Dondi M., The vitreous phase of porcelain stoneware: composition, evolution during sintering and physical properties. *Journal of Non-Crystalline Solids*, 357 (2011) 3251-3260.
- [5] Restrepo J.J., Dinger D.R., Study of the reactions during the firing of a whiteware. *Ceram. Eng. Sci. Proc.*, 14 [1-2] (1993) 116-125.
- [6] Porte F., Brydson R., Rand B., Riley F.L., Creep Viscosity of Vitreous China, *J. Am. Ceram. Soc.*, 87 [5] (2004) 923-928.
- [7] Bernardin A.M., de Medeiros D.S., Riella H.G., Pyroplasticity in porcelain tiles, *Materials Science and Engineering A* 427 (2006) 316-319.
- [8] Raimondo M., Zanelli C., Guarini G., Dondi M., Fabbroni R., Cortesi T., Process of pyroplastic shaping for special-purpose porcelain stoneware tiles. *Ceramics International*, 35 (2009) 1975-1984.
- [9] Tunçel D.Y., Kara M.K., Özel E., Effect of the Chemical Composition on The Pyroplastic Deformation of Sanitaryware Porcelain Body, *IOP Conf. Series: Materials Science and Engineering* 18 (2011) 222025.
- [10] Gualtieri A.F., Accuracy of XRPD QPA using the combined Rietveld-RIR method. *J. Appl. Cryst.* 33 (2000) 267-278.
- [11] Paganelli M., Sighinolfi D., The optical fleximeter to study deformations on ceramics. *Ind. Ceram.* 29 (2009) 1-6.
- [12] Lee S.-H., Messing G.L., Green D.J., Bending Creep Test to Measure the Viscosity of Porous Materials during Sintering. *J. Am. Ceram. Soc.* 86 (2003) 877-882.